Article

Using OCO-2 Satellite Data for Investigating the Variability of Atmospheric CO_2 Concentration in Relationship with Precipitation, Relative Humidity, and Vegetation over Oman

Foroogh Golkar [1], Malik Al-Wardy [2,*], Seyedeh Fatemeh Saffari [3], Kathiya Al-Aufi [2] and Ghazi Al-Rawas [4]

[1] Department of Water Engineering, Oceanic and Atmospheric Research Center, College of Agriculture, Shiraz University, Shiraz 8178757449, Iran; fgolkar@shirazu.ac.ir

[2] Department of Soils, Water, and Agricultural Engineering, Sultan Qaboos University, Muscat PC123, Oman; kathiyaali89@gmail.com

[3] Faculty of Engineering Science, University of Tehran, Tehran 1665737813, Iran; sheida.saffari74@gmail.com

[4] Department of Civil and Architectural Engineering, Sultan Qaboos University, Muscat PC123, Oman; ghazi@squ.edu.om

* Correspondence: mwardy@squ.edu.om

Abstract: Recognition of the carbon dioxide (CO_2) concentration variations over time is critical for tracing the future changes in climate both globally and regionally. In this study, a time series analysis of atmospheric CO_2 concentration and its relationship with precipitation, relative humidity (RH), and vegetation is investigated over Oman. The daily XCO_2 data from OCO-2 satellite was obtained from September 2014 to March 2019. The daily RH and precipitation data were also collected from the ground weather stations, and the Normalized Difference Vegetation Index was obtained from MODIS. Oman was studied in four distinct regions where the main emphasis was on the Monsoon Region in the far south. The CO_2 concentration time series indicated a significant upward trend over different regions for the study period, with annual cycles being the same for all regions except the Monsoon Region. This is indicative of RH, precipitation, and consequently vegetation cover impact on atmospheric CO_2 concentration, resulting in an overall lower annual growth in the Monsoon Region. Simple and multiple correlation analyses of CO_2 concentration with mentioned parameters were performed in zero to three-month lags over Oman. They showed high correlations mainly during the rainfall period in the Monsoon Region.

Keywords: OCO-2 satellite; CO_2 concentration; relative humidity; precipitation; NDVI

1. Introduction

Increases in greenhouse gases, particularly carbon dioxide (CO_2), have accelerated the rise in global air temperatures in recent years [1]. Forster et al. showed that the global mean concentration of CO_2 and the atmospheric radiative forcing associated with it increased to a substantial degree within the last two centuries, causing further disruption in the earth's energy budget balance [2]. The atmospheric radiative forcing changes cause alterations in the atmospheric heating distribution by trapping additional heat, resulting in changes in the different elements of the hydrological cycle and atmospheric moisture content [3], which are subsequently expected to affect precipitation [4–6]. At the same time, precipitation, water vapor content [7], and consequently, vegetation cover have a direct effect [8] on the monthly CO_2 concentration fluctuations.

In the Intertropical Convergence Zone (ITCZ), summer monsoons contribute to the major portion of annual total precipitation in these regions. In this regard, the possible changes in monsoon precipitation with the increase in carbon dioxide concentration have been considered by several researchers [9–11]. Richardson et al. research demonstrated that rapid warming of the land surface is caused by increased CO_2 concentration, resulting in enhanced convection [12], and thus higher precipitation over land in this zone. Loo et al. study also showed an increase in precipitation anomalies beyond the 1970s in the monsoon regions, corresponded with global warming and temperature anomalies' increase in recent decades [9]. This increase subsequently affects land vegetation growth and greenness during the monsoon, resulting in more atmospheric CO_2 absorption and decrease [5]. These interactions cause an annual cycle in CO_2 concentration with seasonal fluctuations [13]. Gupta et al. study showed a strong anti-correlation between the annual cycle of vegetation and mid-tropospheric CO_2 concentration over India [13]. However, high CO_2 concentration in April and May (pre-monsoon period) is explained by the high planetary boundary layer height in these months.

In addition, studies show a strong interaction between CO_2 concentration and atmospheric humidity. Dessler et al. showed that with an increased level of CO_2 concentration, a warmer surface, and hence a more humid troposphere are expected [14]. On the other hand, humidity plays a crucial role in atmospheric CO_2 mixing and its annual cycle [15,16]. In this regard, some studies on global and regional scales have investigated the CO_2 fluctuations with precipitation and relative humidity (RH) [12,15,17–19]. Huang et al. study in monsoon regions indicated that the changes which occur in atmospheric CO_2 levels are related to the thermodynamic components driven by changes in the water vapor [10]. Besides, Wang et al. showed the sensitivities of monthly variability in atmospheric CO_2 concentration with temperature and precipitation using CO_2 records from the Mauna Loa Observatory, Hawaii [7]. The regional study of atmospheric CO_2 concentration changes in association with atmospheric moisture and precipitation is still a challenging question, particularly in regions with scarce rainfall and critical hydrological parameters.

CO_2 concentration data over the world are obtained from ground observation stations as well as ships and aircraft. However, these kinds of measurements are limited to specific locations over the world and are unevenly distributed [1]. Thus, Earth Observation Satellites are used to observe the global CO_2 concentration and to build a detailed spatial distribution of CO_2 sources and sinks [20]. Two types of greenhouse gas observation satellites are used for this purpose, the thermal infrared (TIR) and short-wavelength infrared (SWIR). The TIR measurements are sensitive to CO_2 in the middle and upper troposphere, whereas the SWIR measurements are sensitive to CO_2 in the lower troposphere, where the CO_2 sources and sinks are located [21]. The two main satellites utilizing the SWIR measurements are the Greenhouse Gases Observing Satellite (GOSAT) launched in 2009, and the Orbiting Carbon Observatory (OCO-2) satellite launched in 2014. To improve the understanding of the carbon cycle and to validate the space-based CO_2 concentration, the ground-based Total Carbon Column Observing Network (TCCON) was established in 2004 [22]. This network is composed of "ground-based Fourier transform spectrometers," recording direct solar spectra in the near-infrared bands (TCCON wiki), which is not affected by the surface properties [22]. In this regard, validation of dry air mole fraction of CO_2 (XCO_2) derived from GOSAT in comparison with TCCON shows, in general, a mean bias of less than 2 ppm [1,21,23], providing reliable and valuable information on the variation of CO_2 [23]. Following the same approach, the XCO_2 retrieved from the OCO-2 satellite and its validation with TCCON shows a standard deviation of around 1.3–1.9 ppm and a station-to-station variability of 0.2–0.5 ppm among collocated TCCON sites [1,22–26]. These biases, as shown by Wunch et al. [22], are dependent on latitude, earth surface properties, and scattering by aerosols, although no latitude-dependent bias reported in the ocean and near ocean regions in Wu et al. study [23]. These validations show that despite the slight differences found between the TCCON dry air mole fraction of CO_2 and that of GOSAT and OCO-2, the appropriate spatial resolution and accuracy of these space-based dataset, as well as the relatively long time-series measurement make them suitable for global and regional studies. Several studies utilized data from the two satellites. For

example, Falahatkar et al. investigated the interaction of land surface temperature and Normalized Difference Vegetation Index with GOSAT XCO_2 data for one year over Iran [27], while Fu et al. tracked the fossil fuel consumption in urban areas and revealed the impacts of urban vegetation on seasonal variation of XCO_2 using OCO-2 observations [28]. In addition, Siabi et al. assessed the CO_2 distribution over Iran using XCO_2 data from OCO2 during the growing season [29]. In their study, land cover and wind direction showed the highest impact in CO_2 concentration over Iran. However, no previous studies on CO_2 concentration have been conducted over Oman using ground-based measurements as they lack or space-based observations.

The Sultanate of Oman is a part of Western Asia occupying the southeast of the Arabian Peninsula on the Indian Ocean. The average annual rainfall in the Sultanate of Oman is about 110 mm but can range from <100 to 500 mm [30]. Although July–August is known as the "wet" or "monsoon" period in the south of Oman, this country is one of the most water-stressed regions in the world, and it is relatively sensitive to global climate change [31]. Despite the importance of investigating the atmospheric CO_2 trend in Oman and its monthly variability, no previous studies were carried out, which can be critical in predicting and adapting to the future climate.

Thus, the objectives of the current study can be summarized as analyzing the time series of atmospheric CO_2 concentration over Oman using Earth Observation Satellites as well as investigating the relationship of monthly variability of CO_2 concentration with precipitation along with relative humidity and vegetation cover changes.

2. Materials and Methods

2.1. Study Area

A diverse climate and geography characterize Oman. The terrain varies from the desert plains in the central region to the rugged mountains in the north and south. As for the climate, it is both hot and humid in the northern coastal plains and hot and dry in the central part. In the far south, there is an active southwest summer monsoon in late June to August [30]. Furthermore, because of complex topography, Oman has several local climates across its terrain, according to the Köppen and Geiger classification system varying from dry-arid to semi-arid conditions [32]. As a result, vegetation biomass and distribution are mainly controlled by the low and inconsistent rainfall and the fluctuating temperatures [31]. Therefore, in this study, considering the climate features and the rainfall patterns, Oman is assessed in four distinct regions, as displayed in Figure 1. "Monsoon Region" is referred to the Dhofar Mountains and coastal areas in the southwest with monsoon rainfall pattern and thus exhibit different vegetation cover compared to the rest of Oman. In this region, three distinct periods are considered during the year. Pre-monsoon, covering the period from 1 November to 19 June; monsoon, from 21 June to 30 August; and post-monsoon, from 1 September to 30 October. The second region considered is the "South Region," which despite the slight impact of the monsoon rainfall on this area, still has a different climate and vegetation pattern. The third region, called "Central Region" is located in the center of Oman and is mostly desert with limited rainfall and vegetation. "North Region" is the fourth area that encompasses the northern part of the country, which has varied precipitation and vegetation changing with elevation.

2.2. Dataset

In this study, daily precipitation and RH data are collected from 36 ground weather stations over Oman (Figure 1) for the study period from September 2014 to May 2019. As shown in Figure 1, there is a sufficient number of stations for each of the four study regions and the appropriate distribution of stations over Oman.
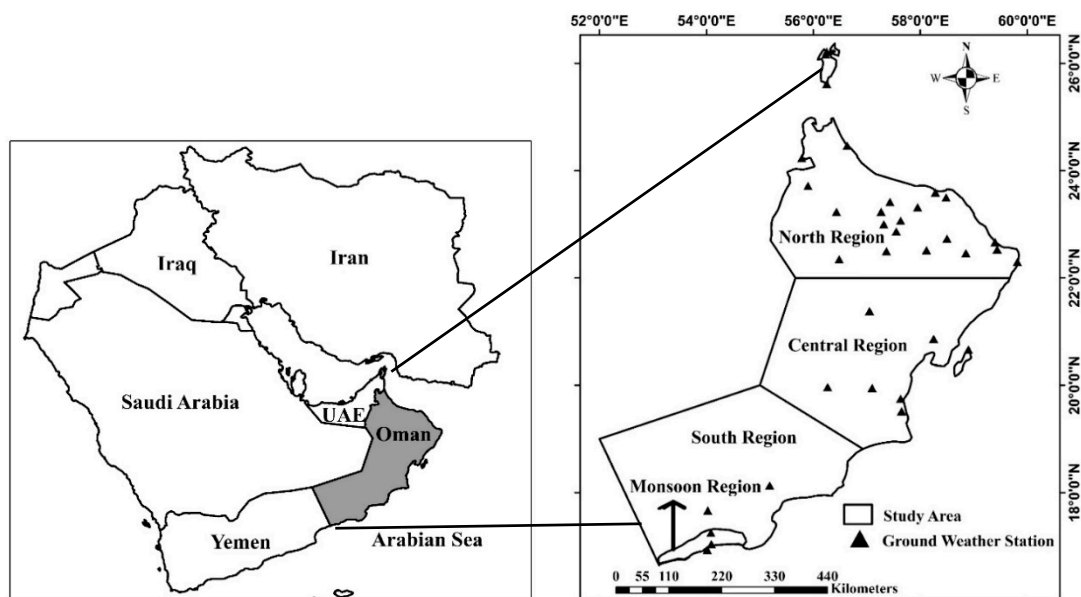
Figure 1. The four study regions with ground weather station locations over Oman.

Because of ground CO_2 observations absence in Oman, the column-averaged CO_2 dry air mole fraction, XCO_2 (hereafter, CO_2 concentration), from the Orbiting Carbon Observatory 2 satellite is obtained in the current study for the period from September 2014 to May 2019 (Daily bias-corrected OCO2_L2_Lite_FP.9r products were downloaded from https://disc.gsfc.nasa.gov). OCO-2 was launched in July 2014 and started providing data in September 2014, intending to estimate CO_2 with high precision and resolution to characterize sources and sinks of this critical greenhouse gas [1,22–24,26]. The satellite flies in a sun-synchronous orbit at an average altitude of 705 km above the earth's surface, with a descending node at around 13:30 local time, at a spatial resolution of roughly 3 km^2 and a temporal resolution of 16 days [26]. Validation of the OCO-2 data set versus measurements from the TCCON, as reported by Wunch et al. [22], shows regional biases of around 0.5 ppm and standard deviations of 1.5 ppm (similar results obtained from other studies in different regions [1,23,26]). These errors, as mentioned by Kaluwik et al. [24], are not entirely due to OCO-2, but TCCON, as well as colocation errors, are also contributing. For this study, the XCO_2 data from Greenhouse gases Observing Satellite (GOSAT) with a more extended period from May 2009 was also considered (Daily Level 2 GOSAT bias-corrected products from https://disc.gsfc.nasa.gov). However, it showed very few numbers of overpasses (23 points) over Oman from 2009 to 2016, while the number of OCO-2 total measurements over Oman during the mentioned period is 473,618 points. Figure 2 shows the OCO-2 measurement points over Oman for the year 2015 as a sample of the satellite overpasses.

With a spatial resolution of 500 m, the Normalized Difference Vegetation Index (NDVI) products from MODIS (Moderate Resolution Imaging Spectroradiometer) images were used for monitoring the overall changes of vegetation over Oman during the study period. The MODIS MCD43A4 Version 6 data used here was extracted and processed over the four study regions using the JavaScript code editor in the GEE (google earth engine) platform. This MODIS dataset is produced daily using 16 days of Terra and Aqua MODIS data temporally weighted to the ninth day (https://lpdaac.usgs.gov/products/mcd43a4v006/). Generally, the NDVI ranges from −1 to +1. The negative values of vegetation index correspond to water, snow, and ice cover. In contrast, bare land value is almost zero, and the typical range of 0.1 and higher is linked with the greenness of plant canopies [33].
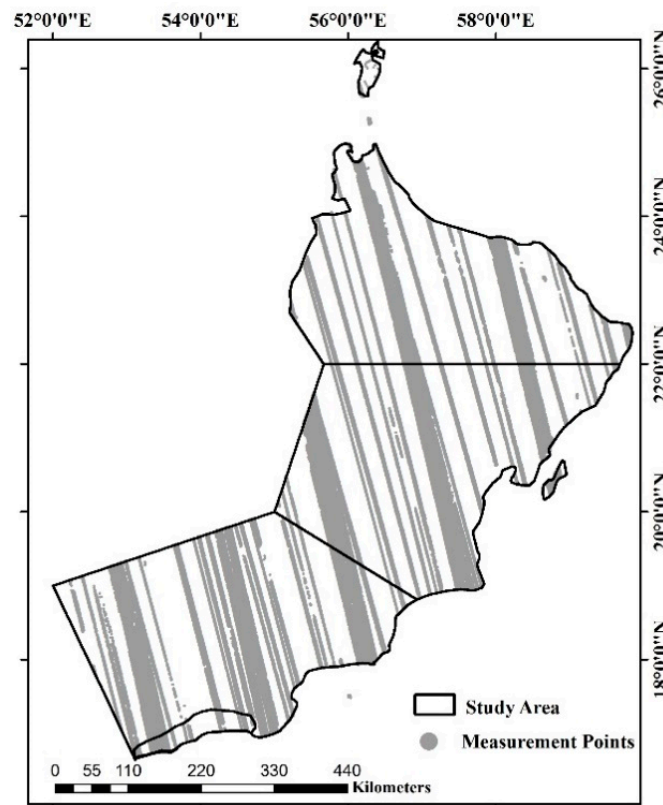
Figure 2. XCO_2 measurement points from OCO-2 overpasses in Oman during 2015.

2.3. Methods

During the study period, the spatial daily and monthly means of CO_2 concentration were calculated based on the satellite passes over each region. The spatial mean of NDVI for the available days was also calculated using GEE for all four study regions. The spatial daily and monthly mean of RH, as well as daily mean and monthly sum of precipitation, were also calculated based on the stations located in each region over the study period.

Time-series analysis is a suitable way to investigate the variation of parameters over time. In this study, the trend analysis of CO_2 concentration as well as precipitation, RH, and NDVI was considered for the four regions over Oman. Simple linear regression (SLR) was applied to test the linear trend, with CO_2 concentration as well as precipitation, RH, and NDVI considered as the dependent variables in the SLR. Also, the non-parametric Mann Kendal test (M-K test) for trend analysis was applied here to identify the significant upward or downward trend of the mentioned parameters. The M-K test, developed by Mann [34] and Kendall [35], statistically detects monotonic increasing or decreasing trends of a variable of interest in a series of data. In this test, the null (H_0) and alternative hypotheses (H_1) identify the absence or presence of a trend in the time series of the investigated data, respectively. The following equations give the M-K test statistic S and the standardized test statistic Z_{MK} used for testing the hypotheses [36]:

$$S = \sum_{i=1}^{n-1} \sum_{j=i+1}^{n} sgn\left(X_j - X_i\right) \tag{1}$$

$$sgn\left(Xj - Xi\right) = \left\{ \begin{array}{ccc} +1 & if & (Xj - Xi) > 0 \\ 0 & if & (Xj - Xi) = 0 \\ -1 & if & (Xj - Xi) < 0 \end{array} \right\} \tag{2}$$

$$Var\left(S\right) = \frac{1}{18}\left[n(n-1)(2n+5) - \sum_{p=1}^{g} t_p\left(t_p - 1\right)\left(2t_p + 5\right)\right] \tag{3}$$

$$Z_{MK} = \begin{cases} \frac{S-1}{\sqrt{Var(S)}} & if \quad S > 0 \\ 0 & if \quad S = 0 \\ \frac{S+1}{\sqrt{Var(S)}} & if \quad S < 0 \end{cases} \tag{4}$$

where X_i and X_j denote the successive data values of the time series collected over the years at times i and j, n is the length of the time series, t_p is the number of observations for the pth value, and g is the number of tied values. Positive values of Z_{MK} indicate that the observed data increase with time, while negative Z_{MK} values indicate data decreasing in the time series. When $|Z_{MK}| > Z_{1-\alpha/2}$, the null hypothesis is rejected and the alternative is accepted indicating a significant existence of a trend in the time series. The statistically significant trend was evaluated in a two-tailed M-K test at a probability level of 0.95 ($\alpha = 0.05$).

Multiple correlation analysis (MCA) was applied in this study to analyze the interaction and the strength of the relationship between CO_2 concentration with precipitation and relative humidity. MCA is commonly used to explain the association between one continuous variable and two or more response variables [37] using a linear function of a set of variables which generalizes the standard coefficient of correlation. It should be mentioned, and as discussed by Huberty [37], there is a distinction between the multiple regression analysis (MRA) and MCA. Such that "in predictive research (MRA), the main emphasis is on practical applications, whereas in explanatory research (MCA), the main emphasis is on understanding phenomena [37]." However, as explained by [37], an initial choice of the response variables for an MCA study should be conducted based on some relevant substantive theory. Here, the response variables were chosen based on the initial simple correlation analysis. Then, the correlation coefficient Equation (5) and p-value of 0.95 probability level are used to test the statistical significance of MCA. However, some response variables have been deleted as a result of low/no contribution to explain the variability.

$$\text{correlation coefficient} = \frac{n \sum_{i=1}^{n} hatY_i \, Y_i - \left(\sum_{i=1}^{n} hatY_i \right)\left(\sum_{i=1}^{n} Y_i \right)}{\sqrt{n \, \sum_{i=1}^{n} hatY_i^2 - \left(\sum_{i=1}^{n} hatY_i \right)^2} \, \sqrt{\sqrt{n \, \sum_{i=1}^{n} Y_i^2 - \left(\sum_{i=1}^{n} Y_i \right)^2}}} \tag{5}$$

where Y_i and $hatY_i$ are response variable and continuous variable values, respectively.

3. Results and Discussion

3.1. Time Series Analysis and Monthly CO_2 Concentration Variability along with Other Parameters

The monthly CO_2 concentration time series for different regions in Oman, as well as the fitted linear regressions, are plotted in Figure 3 for the whole study period from September 2014 to May 2019. The CO_2 concentration is shown to be increasing for all the regions under study with an estimated slope of 0.19 to 0.23 ppm/month (Figure 3). The M-K test for trend analysis of CO_2 concentration showed a significant upward trend for all regions but with a sharper increase in the Central and North Regions. It should be mentioned here that the trend analysis was performed for RH, precipitation, and NDVI over the different regions in Oman and showed a significant positive trend of RH for the Monsoon and South Regions, while no significant trend was found for precipitation and NDVI for all regions in Oman. Figure 3 shows that the Monsoon Region is marked by more intense fluctuations during the study period, with sharp decreases in CO_2 concentration levels in some months of this region, while other regions show smoother fluctuations. These sharp decreases in CO_2 concentrations in these months characterizes the lower annual growth in CO_2 concentrations not only in the Monsoon region but the South region as a whole. Thus, to explore these differences and for better comparison, the monthly CO_2 concentration time series is plotted against monthly precipitation as well as RH and NDVI to show the CO_2 fluctuation in association with other parameters (Figure 4). In general, there seems to be an association between CO_2 concentration and RH on a monthly basis, as higher peaks of

CO_2 concentration seem to coincide with lower peaks of RH in all regions. The same pattern applies to CO_2 concentration and NDVI in the Monsoon and South Regions, but the influence of time lags is detected here. This association between CO_2 concentration and NDVI is not visible in other regions because of the sparse vegetation cover and the fact that a large part of these regions is mainly deserts. The interaction between monthly mean carbon dioxide concentration and monthly precipitation seems to be more complicated to be discussed based on the graphs in Figure 4. Hence, for more precise comparison, the climatology mean (CM) of monthly CO_2 concentration in association with CM of monthly RH and NDVI and particularly precipitation is investigated.
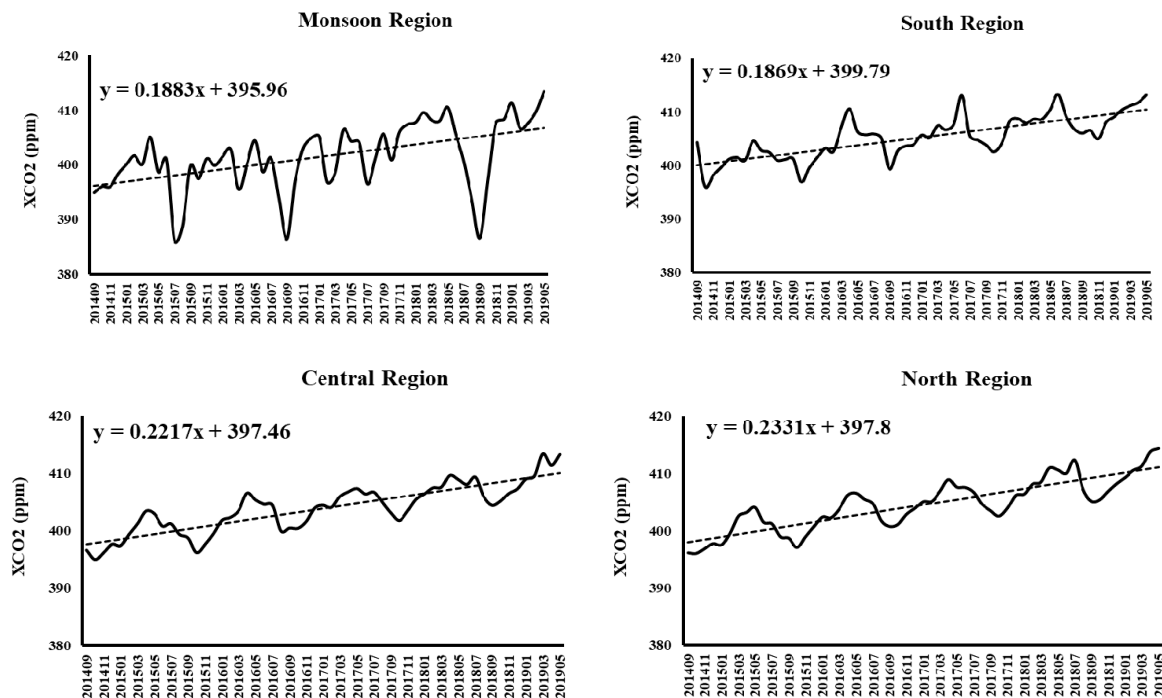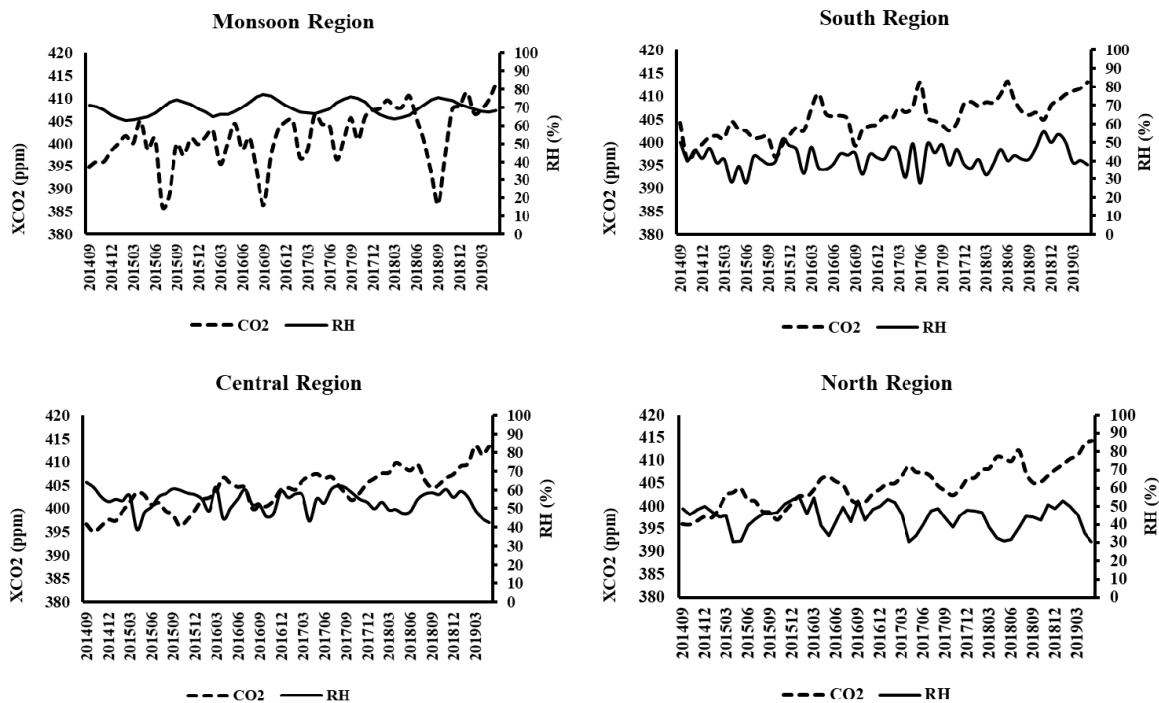

Figure 3. Monthly CO_2 time series for different regions in Oman for the period September 2014 to May 2019. The dashed line indicates the corresponding linear trend.

The CM for monthly CO_2 concentration during the study period for the four regions is plotted in Figure 5. The monthly variation for all regions excluding the Monsoon Region ranges from 399 to 408 ppm, while for the Monsoon Region it ranges from 388 to 407 ppm. The CO_2 concentration for all regions except the Monsoon Region is lowest in October and highest in April. In the Monsoon Region, however, the CO_2 concentration starts decreasing in January, reaching the first minimum (402 ppm) in March and then increases slightly in April and drops again in August during the monsoon period to 388 ppm. To study and clarify the monthly changes of CO_2 concentration, 3Y axes CM of monthly CO_2 concentration, precipitation, and RH as well as 3Y axes CM of monthly CO_2 concentration, precipitation and NDVI are plotted and shown in Figure 6. Based on Figure 6, the sharp decrease in CO_2 concentration in the Monsoon Region in August occurred simultaneously with the highest precipitation, RH, and NDVI during the monsoon period, though there are time lags between minimum CO_2 concentration and maximum NDVI. In other words, during the monsoon season, there is an increase in relative humidity and precipitation and subsequently vegetation, which eventually causes a decrease in CO_2 concentration in this region. There is a decrease in CO_2 concentration in March, and although it does not seem to be linked with precipitation, RH, or NDVI within the boundary of monsoon region, it seems that there might be an impact of precipitation in the vicinity of this region on CO_2 concentrations as ground stations close by in the south region have recorded especially high precipitation in the Month of March (Figure 6). This decrease in CO_2 concentration could be

associated with other parameters related to regional land characteristics as well, but this needs to be further investigated.

(**a**)

(**b**)
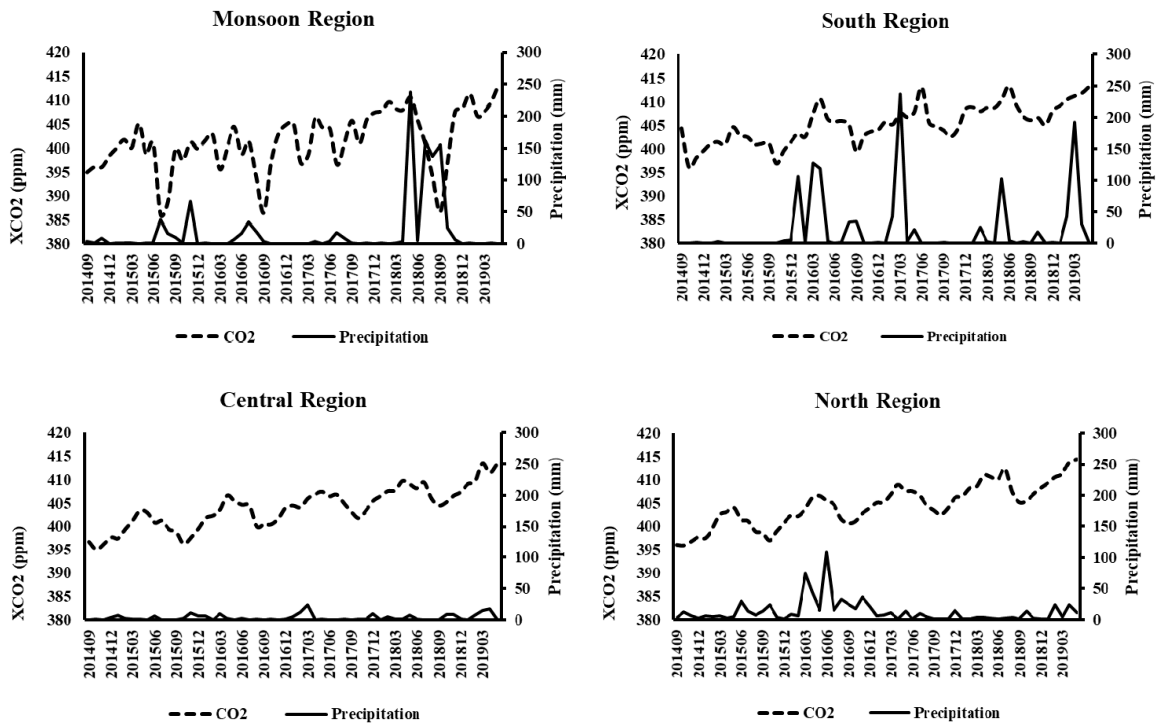
Figure 4. *Cont.*
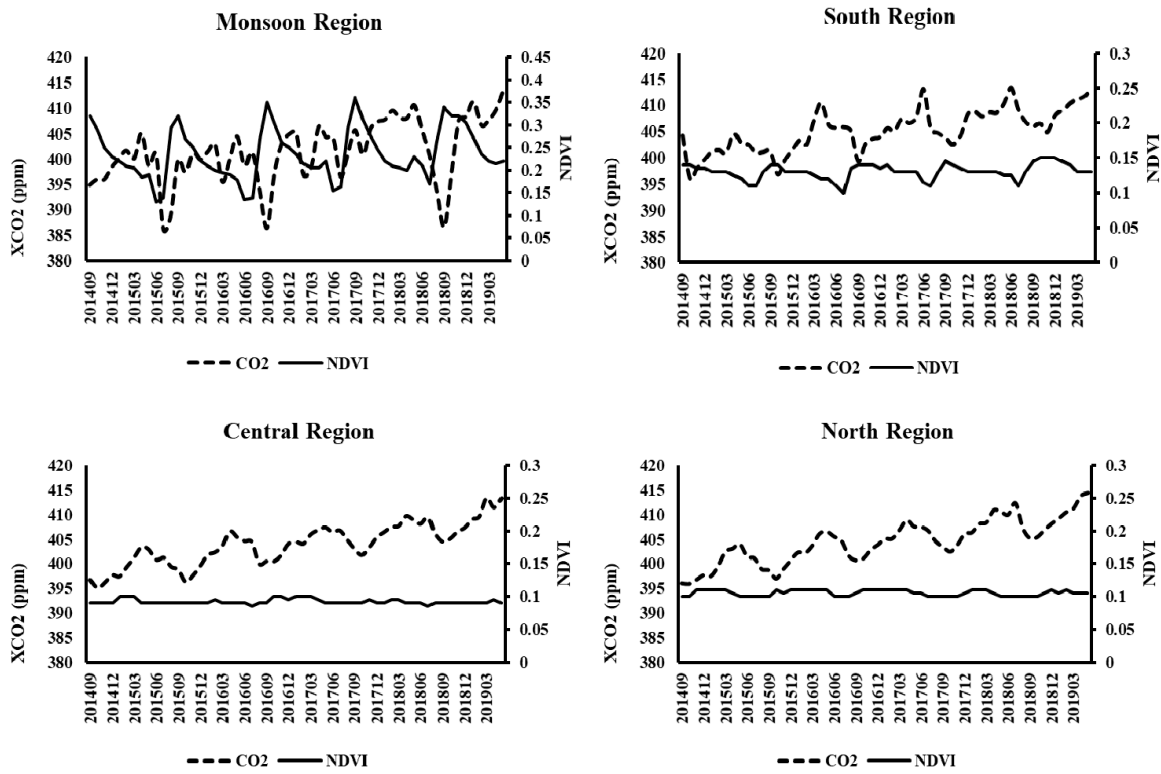
Figure 4. Monthly CO_2 time series fluctuations against (**a**) precipitation, (**b**) relative humidity (RH), and (**c**) Normalized Difference Vegetation Index (NDVI) for different regions in Oman for the period September 2014 to May 2019.
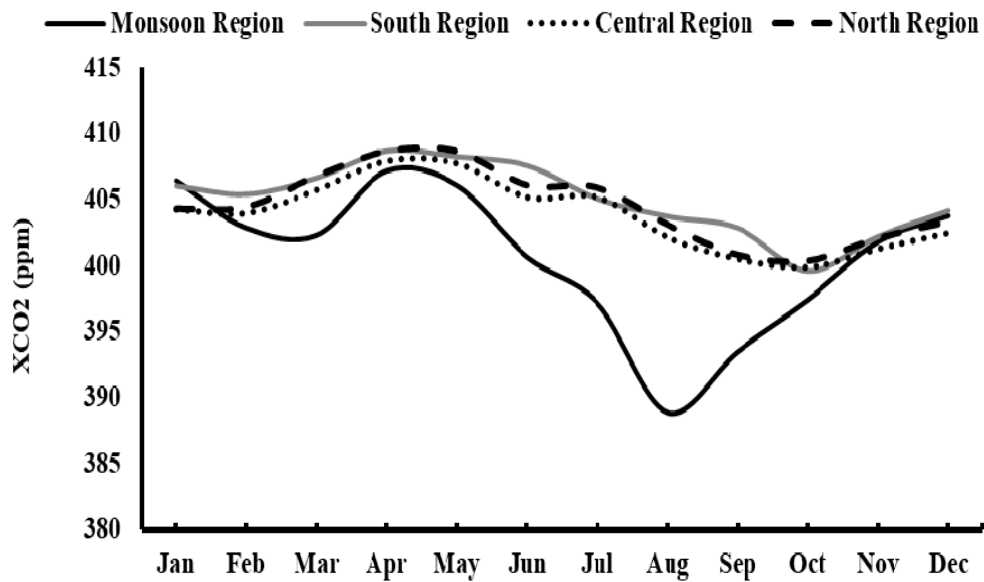
Figure 5. Climatology mean (CM) of monthly CO_2 concentration over the four study regions of Oman.
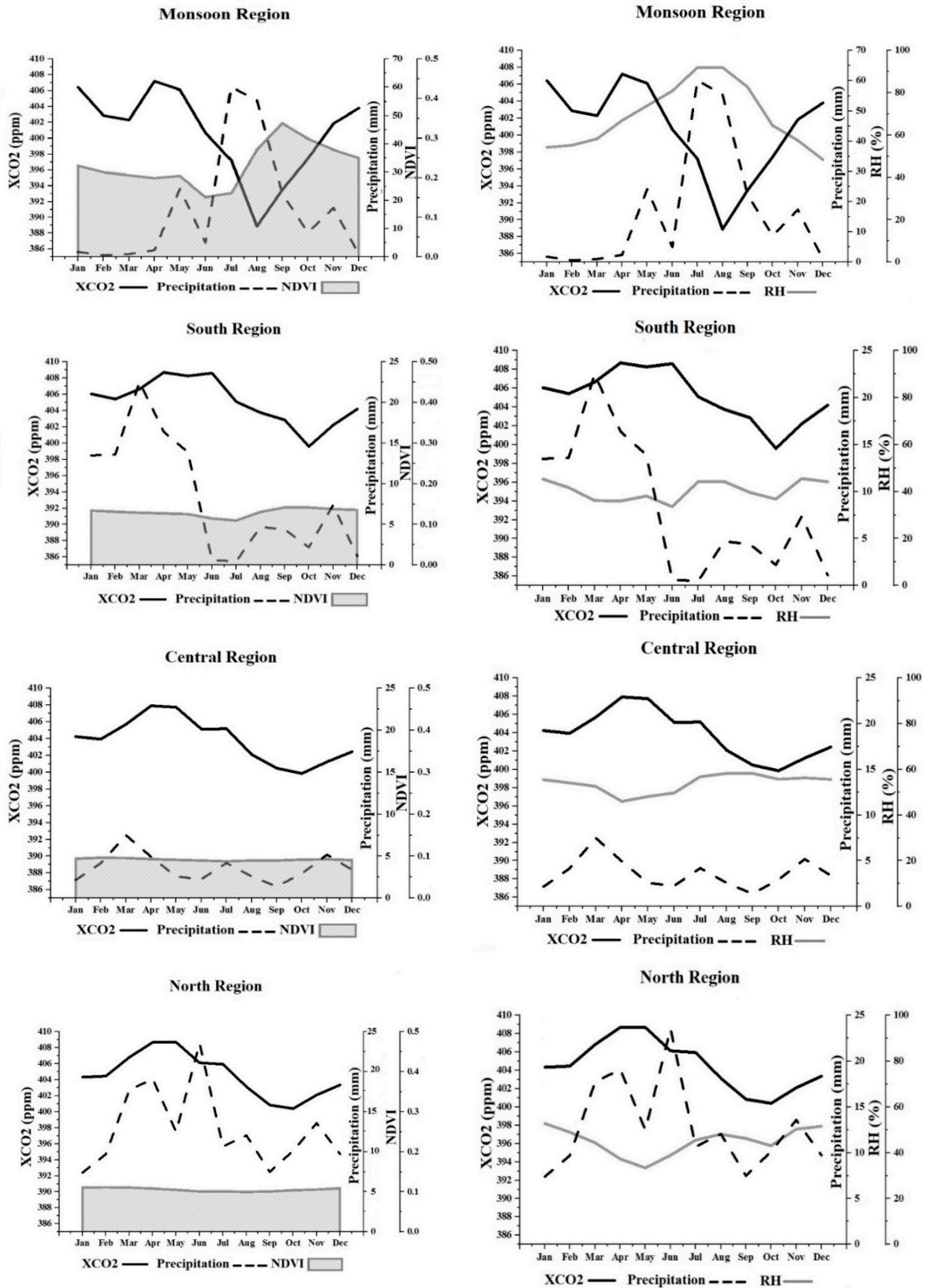
Figure 6. 3Y axes plot of CM of monthly CO_2 and precipitation vs. NDVI or RH.

3.2. CO$_2$ Concentration Relationship with Other Parameters

In this section, the correlation between CO$_2$ concentration, relative humidity, and precipitation, using daily records on a monthly basis is investigated. Because of the limited number of NDVI data each month, this parameter is not taken into consideration here. It should also be mentioned that for precipitation data, only days with recorded rainfall are included in the correlation with coinciding days of other parameters. Because of the different characteristics of the Monsoon Region, a detailed correlation investigation was performed, and the same procedure was then applied to other regions.

Linear correlation analysis of CO$_2$ concentration with precipitation in the Monsoon Region showed a negative correlation coefficient for all months, which indicates atmospheric CO$_2$ decline because of precipitation [7]. The correlation coefficients for this region are presented in Figure 7. In this study, only the months of January to April, as well as June, have shown a non-significant correlation based on *p*-values of $\alpha = 0.05$. Here, the lack of continuous days with significant precipitation can be the reason for the insignificant correlation.
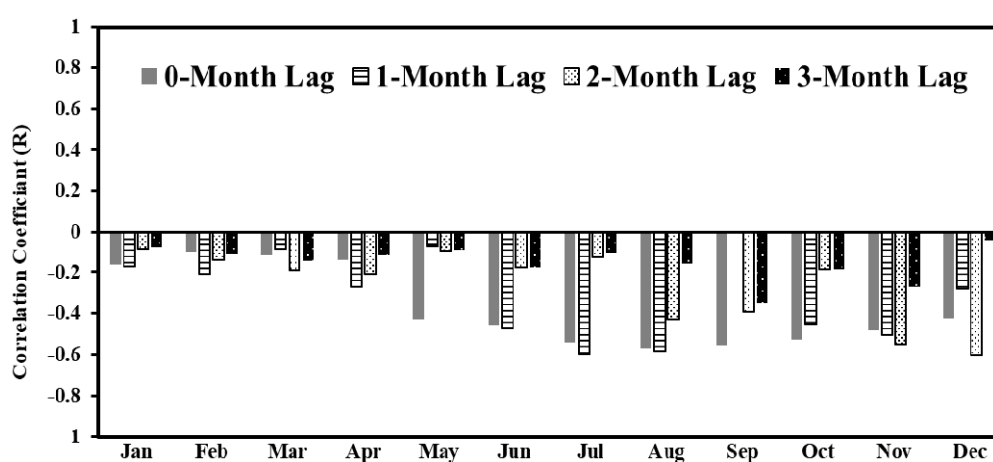
Figure 7. The CO$_2$-precipitation correlation coefficients in the Monsoon Region.

The daily CO$_2$ concentration correlation with precipitation was investigated with one, two, and three-month lags. This was done to evaluate the possible effect of monthly time lags on the consequent month's CO$_2$ concentration. This analysis showed a significant CO$_2$-precipitation relationship with one to three-month lags for some periods in the Monsoon region. Significant correlations in different time lags based on a *p*-value of $\alpha = 0.05$ are shown in Figure 8. These results show that an increase in precipitation in June, July, and August results in a decrease in CO$_2$ concentration of the following months. The same applies for September and October precipitation. A significant two-month lag correlation in CO$_2$ concentration was also seen with precipitation in August and September, and a significant three-month lag correlation with September rainfall.

In a research done by [7] for investigating the monthly variability in atmospheric CO$_2$ growth rate in Mauna Loa, air temperature and precipitation correlation with carbon dioxide concentration changes with 1 to 12-month lags were considered. As a result, significant correlations in 4-month lag in precipitation and 1-month lag for temperature with CO$_2$ growth rate were reported in their study. To further explain our recent findings, it can be added that along with rainy days' impact on the CO$_2$ concentration decrease of the same month, the effect of the previous month's rainfall on vegetation and, consequently, carbon dioxide absorption can be considered as another factor.

Monsoon Region

	Lag	Jan	Feb	Mar	Apr	May	Jun	Jul	Aug	Sep	Oct	Nov	Dec
CO2-Precipitation	0					*		*	*	*	*	*	
	1						*	*	*	*	*		
	2								*	*			
	3									*			
CO2-RH	0				*	*	*	*	*	*	*	*	*
	1	*			*	*	*	*	*	*		*	*
	2				*	*	*	*	*	*			*
	3								*	*			

South Region

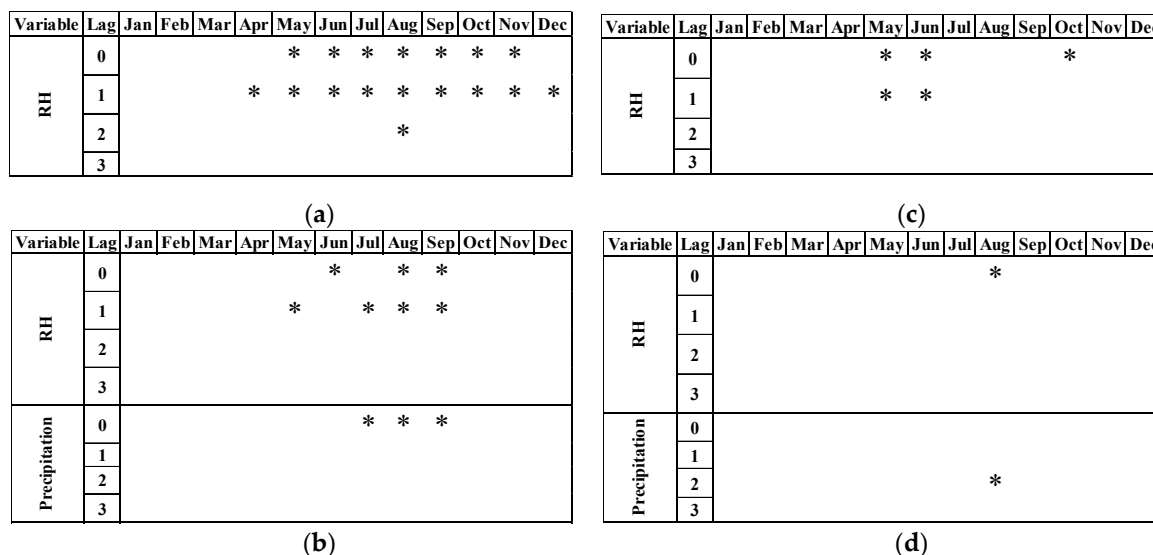|	Lag	Jan	Feb	Mar	Apr	May	Jun	Jul	Aug	Sep	Oct	Nov	Dec
CO2-Precipitation	0												
	1		*										
	2							*					
	3												
CO2-RH	0						*	*					
	1												
	2												
	3												

Central Region

	Lag	Jan	Feb	Mar	Apr	May	Jun	Jul	Aug	Sep	Oct	Nov	Dec
CO2-Precipitation	0												
	1												
	2												
	3												
CO2-RH	0				*								
	1				*								
	2												
	3												

North Region

	Lag	Jan	Feb	Mar	Apr	May	Jun	Jul	Aug	Sep	Oct	Nov	Dec
CO2-Precipitation	0												
	1												
	2								*				
	3									*			
CO2-RH	0		*	*	*	*	*	*	*		*		
	1						*	*			*		
	2												
	3												

Figure 8. Significant simple correlations in CO_2, precipitation and RH over Oman, the stars are marked in desired month for carbon dioxide.

Furthermore, monthly carbon dioxide concentration correlation with relative humidity as well as one-month to three-month lags is investigated in this study. The CO_2-RH correlation with lags is performed to test the possible impact of the preceding month's relative humidity on the carbon dioxide concentration of each month. Significant negative CO_2-RH correlations are detected during the year except for January, February, April, and May (Figure 8). Meanwhile, significant correlations in one-month lag are recognized throughout the year except for February, March, and October. Significant correlations for two and three-month lags are also shown in Figure 8. However, the CO_2-RH association is not similar across the two and three-month lags varying between positive and negative correlations, where the negative correlation coefficients were more frequent. This could be related to complex atmosphere thermodynamic components of relative humidity and its interaction with precipitation [10].

As it is presented in Figure 8, the same approach was applied for the three remaining regions of Oman. More stable atmospheric conditions with rare rainy days during the year, less relative humidity changes, and less fluctuation in CO_2 concentration can be the reason for fewer months with significant correlation in South and Central regions, particularly in correlations involving precipitation. However, in the North Region, there are more months with significant correlations that reflect the impact of regional interaction of precipitation and RH on CO_2 fluctuation due to different topography features and rainfall patterns. In general, along with the global increase in carbon dioxide as well as its increasing trend over Oman, the points discussed above highlight the impact of regional atmospheric conditions on CO_2 concentration changes, particularly in the Monsoon Region.

Therefore, defining multiple correlation analysis between CO_2 and precipitation as well as RH in the months with more than one significant correlation is considered. This attempt aims to obtain a multivariate relationship to justify the interaction of different parameters on local carbon dioxide fluctuations. It should be mentioned that in MCA, the main emphasis is on understanding interactions, which explain the relationship between a single variable and a collection of response variables [37]. Predicting regional CO_2 concentration fluctuations is not the purpose of this study.

Here, the CO_2 concentration interaction with multiple variables, including precipitation and RH in different time lags for the Monsoon Region as the region with a higher number of months with significant correlations, was investigated. It is worth to mention that two sets of MCA are considered. The first is the MCA of CO_2-RH, which is carried out for all days with data (Figure 9a), and the second is the MCA of CO_2-RH-precipitation, where only days with precipitation are considered (Figure 9b).

(a)

Variable	Lag	Jan	Feb	Mar	Apr	May	Jun	Jul	Aug	Sep	Oct	Nov	Dec
RH	0					*	*	*	*	*	*	*	
	1				*	*	*	*	*	*	*	*	*
	2							*					
	3												

(c)

Variable	Lag	Jan	Feb	Mar	Apr	May	Jun	Jul	Aug	Sep	Oct	Nov	Dec
RH	0					*	*			*			
	1					*	*						
	2												
	3												

(b)

Variable	Lag	Jan	Feb	Mar	Apr	May	Jun	Jul	Aug	Sep	Oct	Nov	Dec
RH	0						*		*	*			
	1					*			*	*			
	2												
	3												
Precipitation	0							*	*	*			
	1												
	2												
	3												

(d)

Variable	Lag	Jan	Feb	Mar	Apr	May	Jun	Jul	Aug	Sep	Oct	Nov	Dec
RH	0								*				
	1												
	2												
	3												
Precipitation	0												
	1												
	2									*			
	3												

Figure 9. Significant months and variables in MCA, (**a**) Monsoon Region CO_2-RH MCA, (**b**) Monsoon Region CO_2-RH-precipitation MCA, (**c**) North Region CO_2-RH MCA, (**d**) North Region CO_2-RH-precipitation MCA.

The multiple correlation analysis shows that the existence of a significant simple correlation between CO_2 and another variable, for example, in August for the Monsoon Region (Figure 8), is not necessarily confirmed in a multivariate correlation (Figure 9a,b). Also, the existence of multiple significant correlations between CO_2 and other variables, for example, in the Monsoon Region in October (Figure 8), does not necessarily lead to the definition of a significant MCA in the same month (Figure 9b). In other words, some response variables which had a significant impact on simple correlation were insignificant in MCA, which could be due to the interaction between the response variables.

Figure 9 also shows significantly correlated variables for months with acceptable MCAs. As it is shown in Figure 9a, if only RH is considered in MCA, it will be possible to establish multivariate correlations for a longer period from May to November, which reveals more significant correlations in the monsoon period. Besides, RH with zero and one-month lags are recognized as more effective variables in local carbon dioxide fluctuation, whereas two-month and three-month lags have been eliminated in most of the months. At the same time, when both RH and precipitation are involved in MCA (Figure 9b), the period with significant MCA is limited to the months with more frequent rainy days. As a result, in MCAs including days with both RH and precipitation, RH displays less impact on carbon dioxide fluctuations compared to when it is considered individually. Furthermore, fewer correlation coefficients are obtained in months when both RH and precipitation are involved in MCA.

In the North Region, multiple correlations in CO_2-RH analysis (Figure 9c) were significant in May and June for zero and one-month lags, whereas only in August, a significant MCA with RH and three-month lag precipitation is established (Figure 9d).

4. Conclusions

In this study, because of the lack of ground-based measurements, the CO_2 concentration data captured by the OCO-2 satellite was used. The trend analysis of CO_2 concentration during the study period shows a significant upward trend all over Oman. However, the Monsoon Region shows a lower increasing rate but more interannual variations. Along with being aware of the global upward trend and seasonal cycle of CO_2, the effects of regional characteristics such as precipitation, relative humidity, and vegetation on monthly fluctuations of CO_2 were considered over Oman. This research showed that in the Monsoon Region with higher precipitation as well as higher relative humidity and vegetation cover, the monthly atmospheric CO_2 concentrations were significantly affected by the regional parameters compared to the rest of Oman. Precipitation was shown to have a higher impact in defining the changes in CO_2 concentrations. Ultimately, despite the short study period, the findings of current research are sound and reliable. However, other parameters such as soil temperature and soil moisture relationship with atmospheric CO_2 concentration variations are suggested in further studies.

Author Contributions: F.G. and M.A.-W. performed the data processing and analysis, and wrote the original draft; S.F.S. participated in data analysis and literature review; K.A.-A. participated in GIS mapping; and G.A.-R. participated in review and editing. All authors have read and agreed to the published version of the manuscript.

Conflicts of Interest: The authors declare no conflict of interest.

References

1. Kong, Y.; Chen, B.; Measho, S. Spatio-temporal consistency evaluation of XCO_2 retrievals from GOSAT and OCO-2 based on TCCON and model data for joint utilization in carbon cycle research. *Atmosphere* **2019**, *10*, 354. [CrossRef]

2. Forster, P.; Ramaswamy, V.; Artaxo, P.; Berntsen, T.; Betts, R.; Fahey, D.W.; Haywood, J.; Lean, J.; Lowe, D.C.; Myhre, G.; et al. Changes in Atmospheric Constituents and in Radiative Forcing. In *Climate Change 2007 the Physical Science Basis. Contribution of Working Group I to the Fourth Assessment Report of the Intergovernmental Panel on Climate Change*; Cambridge University Press: Cambridge, UK; New York, NY, USA, 2007.

3. Richter, I.; Xie, S.P. Muted precipitation increase in global warming simulations: A surface evaporation perspective. *J. Geophys. Res. Atmos.* **2008**, *113*. [CrossRef]

4. Mitchell, J.F. The seasonal response of ageneral circulation model to changes in CO_2 and sea temperatures. *Q. J. R. Meteorol. Soc.* **1983**, *109*, 113–152. [CrossRef]

5. Allen, M.R.; Ingram, W. Constraints on future changes in the hydrological cycle. *Nature* **2002**, *419*, 224–228. [CrossRef]

6. Held, I.M.; Soden, B.J. Robust responses of the hydrological cycle to global warming. *J. Clim.* **2006**, *19*, 5686–5699. [CrossRef]

7. Wang, J.; Zeng, N.; Wang, M. Interannual variability of the atmospheric CO_2 growth rate: Roles of precipitation and temperature. *Biogeosciences* **2016**, *13*, 2339–2352. [CrossRef]

8. Tiwari, Y.K.; Revadekar, J.V.; Ravi Kumar, K. Variations in atmospheric Carbon Dioxide and its association with rainfall and vegetation over India. *Atmos. Environ.* **2013**, *68*, 45–51. [CrossRef]

9. Loo, Y.Y.; Billa, L.; Singh, A. Effect of climate change on seasonal monsoon in Asia and its impact on the variability of monsoon rainfall in Southeast Asia. *Geosci. Front.* **2015**, *6*, 817–823. [CrossRef]

10. Cherchi, A.; Alessandri, A.; Masina, S.; Navarra, A. Effects of increased CO_2 levels on monsoons. *Clim. Dyn.* **2011**, *37*, 83–101. [CrossRef]

11. Sohn, B.J.; Yeh, S.W.; Lee, A.; Lau, W.K.M. Regulation of atmospheric circulation controlling the tropical Pacific precipitation change in response to CO_2 increases. *Nat. Commun.* **2019**, *10*, 1108. [CrossRef]

12. Richardson, T.B.; Forster, P.M.; Andrews, T.; Doug, J.P. Understanding the rapid precipitation response to CO_2 and aerosol forcing on a regional scale. *J. Clim.* **2016**, *29*, 583–594. [CrossRef]

13. Gupta, A.; Dhaka, S.K.; Matsumi, Y.; Imasu, R.; Hayashida, S.; Singh, V. Seasonal and annual variation of AIRS retrieved CO_2 over India during 2003–2011. *J. Earth Syst. Sci.* **2019**, *128*, 1–12. [CrossRef]

14. Dessler, A.E.; Schoeberl, M.R.; Wang, T.; Davis, S.M.; Rosenlof, K.H. Stratospheric water vapor feedback. *Proc. Natl. Acad. Sci. USA* **2013**, *110*, 18087–18091. [CrossRef] [PubMed]

15. Mahesh, P.; Sreenivas, G.; Rao, P.V.N.; Dadhwal, V.K.; Sai Krishna, S.V.S.; Mallikarjun, K. High-precision surface-level CO_2 and CH_4 using off-axis integrated cavity output spectroscopy (OA-ICOS) over Shadnagar, India. *Int. J. Remote Sens.* **2015**, *36*, 5754–5765. [CrossRef]

16. Sreenivas, G.; Mahesh, P.; Subin, J.; Lakshmi Kanchana, A.; Venkata Narasimha Rao, P.; Kumar Dadhwal, V. Influence of meteorology and interrelationship with greenhouse gases (CO_2 and CH_4) at a suburban site of India. *Atmos. Chem. Phys.* **2016**, *16*, 3953–3967. [CrossRef]

17. Wypych, A.; Bochenek, B.; Rózycki, M. Atmospheric moisture content over Europe and the Northern Atlantic. *Atmosphere* **2018**, *9*, 18. [CrossRef]

18. Bony, S.; Bellon, G.; Klocke, D.; Sherwood, S.; Fermepin, S.; Denvil, S. Robust direct effect of carbon dioxide on tropical circulation and regional precipitation. *Nat. Geosci.* **2013**, *6*, 447–451. [CrossRef]

19. Huang, P.; Xie, S.P.; Hu, K.; Huang, G.; Huang, R. Patterns of the seasonal response of tropical rainfall to global warming. *Nat. Geosci.* **2013**, *6*, 357–361. [CrossRef]

20. Chiba, T.; Haga, Y.; Inoue, M.; Kiguchi, O.; Nagayoshi, T.; Madokoro, H.; Morino, I. Measuring regional atmospheric CO_2 concentrations in the lower troposphere with a non-dispersive infrared analyzer mounted on a UAV, Ogata Village, Akita, Japan. *Atmosphere* **2019**, *10*, 487. [CrossRef]

21. Ishizawa, M.; Mabuchi, K.; Shirai, T.; Inoue, M.; Morino, I.; Uchino, O.; Yoshida, Y.; Belikov, D.; Maksyutov, S. Inter-annual variability of summertime CO_2 exchange in Northern Eurasia inferred from GOSAT XCO_2. *Environ. Res. Lett.* **2016**, *11*, 105001. [CrossRef]

22. Wunch, D.; Wennberg, P.O.; Osterman, G.; Fisher, B.; Naylor, B.; Roehl, M.C.; O'Dell, C.; Mandrake, L.; Viatte, C.; Kiel, M.; et al. Comparisons of the Orbiting Carbon Observatory-2 (OCO-2) XCO_2 measurements with TCCON. *Atmos. Meas. Tech.* **2017**, *10*, 2209–2238. [CrossRef]

23. Wu, L.; Hasekamp, O.; Hu, H.; Landgraf, J.; Butz, A.; Aan De Brugh, J.; Aben, I.; Pollard, D.F.; Griffith, D.W.T.; Feist, D.G.; et al. Carbon dioxide retrieval from OCO-2 satellite observations using the RemoTeC algorithm and validation with TCCON measurements. *Atmos. Meas. Tech.* **2018**, *11*, 3111–3130. [CrossRef]

24. Kulawik, S.S.; O'Dell, C.; Nelson, R.R.; Taylor, T.E. Validation of OCO-2 error analysis using simulated retrievals. *Atmos. Meas. Tech. Discuss.* **2018**, *7*, 1–42. [CrossRef]

25. Eldering, A.; Wennberg, P.O.; Viatte, C.; Frankenberg, C.; Roehl, C.M.; Wunch, D. The Orbiting Carbon Observatory-2: First 18 months of science data products. *Atmos. Meas. Tech.* **2017**, *10*, 549–563. [CrossRef]

26. Crisp, D.; Pollock, H.; Rosenberg, R.; Chapsky, L.; Lee, R.; Oyafuso, F.; Frankenberg, C.; Dell, C.; Bruegge, C.; Doran, G.; et al. The on-orbit performance of the Orbiting Carbon Observatory-2 (OCO-2) instrument and its radiometrically calibrated products. *Atmos. Meas. Tech.* **2017**, *10*, 59–81. [CrossRef]

27. Falahatkar, S.; Mousavi, S.M.; Farajzadeh, M. Spatial and temporal distribution of carbon dioxide gas using GOSAT data over IRAN. *Environ. Monit. Assess.* **2017**, *189*, 627. [CrossRef]

28. Fu, P.; Xie, Y.; Moore, C.E.; Myint, S.W.; Bernacchi, C.J. A Comparative Analysis of Anthropogenic CO_2 Emissions at City Level Using OCO-2 Observations: A Global Perspective. *Earth's Future* **2019**, *7*, 1058–1070. [CrossRef]

29. Siabi, Z.; Falahatkar, S.; Alavi, S.J. Spatial distribution of XCO_2 using OCO-2 data in growing seasons. *J. Environ. Manag.* **2019**, *244*, 110–118. [CrossRef]

30. Kwarteng, A.Y.; Dorvlo, A.S.; Kumar, G.T.V. Analysis of a 27-year rainfall data (1977–2003) in the Sultanate of Oman. *Int. J. Climatol.* **2009**, *29*, 605–617. [CrossRef]

31. Charabi, Y. Projection of Future Changes in Rainfall and Temperature Patterns in Oman. *J. Earth Sci. Clim. Chang.* **2013**, *4*, 1–8. [CrossRef]

32. Kottek, M.; Grieser, J.; Beck, C.; Rudolf, B.; Rubel, F. World map of the Köppen-Geiger climate classification updated. *Meteorol. Z.* **2006**, *15*, 259–263. [CrossRef]

33. James, M.E.; Kalluri, S.N.V. The Pathfinder AVHRR land data set: An improved coarse resolution data set for terrestrial monitoring. *Int. J. Remote Sens.* **1994**, *15*, 3347–3363. [CrossRef]

34. Mann, H.B. Nonparametric Tests Against Trend. *Econometrica* **1945**, *13*, 245–259. [CrossRef]

35. Kendall, M. *Rank Correlation Methods*, 2nd ed.; Griffin: London, UK, 1948.

36. Shadmani, M.; Marofi, S.; Roknian, M. Trend Analysis in Reference Evapotranspiration Using Mann-Kendall and Spearman's Rho Tests in Arid Regions of Iran. *Water Resour. Manag.* **2012**, *26*, 211–224. [CrossRef]

37. Huberty, C.J. Multiple correlation versus multiple regression. *Educ. Psychol. Meas.* **2003**, *63*, 271–278. [CrossRef]